

Tuning to sound frequency in auditory field potentials

Christoph Kayser, Christopher I. Petkov & Nikos K. Logothetis

Max Planck Institute for Biological Cybernetics, Spemannstrasse 38, 72076 Tübingen,
Germany

Corresponding author: C. Kayser, email: Christoph.kayser@tuebingen.mpg.de
phone: +49-7071-601659, fax: +49-7071-601652

Running head: Frequency tuning in auditory field potentials

Abstract

Neurons in auditory cortex are selective for the frequency content of acoustical stimuli. Classically, this response selectivity is studied at the single neuron level. However, current research often employs functional imaging techniques to investigate the organization of auditory cortex. The signals underlying the imaging data arise from neural mass action and reflect the properties of populations of neurons. For example, the signal used for functional magnetic resonance imaging (fMRI-BOLD) was shown to correlate with the oscillatory activity quantified by local field potentials (LFP). This raises the questions of how the frequency selectivity in neuronal population signals compares to the tuning of spiking responses. To address this, we quantified tuning properties of auditory evoked potentials (AEP), different frequency bands of the LFP, analog multi-unit (AMUA) and spike-sorted single- and multi-unit activity in auditory cortex.

The AMUA showed a close correspondence in frequency tuning to the spike-sorted activity. In contrast, for the LFP we found a clear dissociation of high and low frequency bands: there was a gradual increase of tuning-curve similarity, tuning specificity and information about the stimulus with increasing LFP frequency. While properties of the high frequency LFP matched those of spiking activity, the lower frequency bands differed considerably, as did the AEP. These results demonstrate that electrophysiological population responses exhibit varying degrees of frequency tuning and suggest that those functional imaging methods that are related to high frequency oscillatory activity should well reflect the neuronal processing of sound frequency.

Keywords: Auditory cortex, local field potential, MUA, information, response selectivity

Main text

The responses of many neurons in early sensory cortices change systematically when a particular feature of their sensory input is manipulated. Neurons in primary visual cortex, for example, are selective to the orientation or spatial frequency of a visual pattern (Hubel and Wiesel 1962), while neurons in primary auditory cortex are modulated by a sound's frequency spectrum (Merzenich and Brugge 1973). Studying individual neurons' feature selectivity has revealed a spatial organization, in which neighboring neurons have similar preferences and collectively form topographic representations of the respective feature; e.g. a tonotopic map of the cochlear partition in the case of the auditory system (Kaas et al. 1999; Rauschecker et al. 1997). This spatial organization aids the study of this feature selectivity using techniques with lower spatial resolution – such as non-invasive functional imaging methods. With regard to the auditory system, several studies demonstrated that functional imaging can reproduce sound frequency maps in auditory cortex (Formisano et al. 2003; Petkov et al. 2006; Talavage et al. 2004; Wessinger et al. 1997).

In trying to integrate information from complementary methodologies, a basic but important question is the similarity between feature-maps obtained. The signals underlying functional imaging arise from populations of neurons and are a result of neural mass action (Freeman 1975; Logothetis and Wandell 2004). Recent work suggests that the fMRI-BOLD signal reflects the spatially summed somato-dendritic potentials and correlates well with electrophysiological population signals such as the local field potential (LFP) (Lauritzen 2001; Logothetis et al. 2001): especially the high frequency oscillatory activity characterized by the LFP seems to correspond to what is measured by the BOLD signal. To the extent that particular LFP frequency-bands may reflect distinct aspects of local processing, different imaging methods may also reveal diverse aspects of information processing. The driving, stimulus-related properties of the LFPs, including their response tuning, thus require careful examination.

Concerning the auditory system, electrophysiological population responses are only little investigated with regard to sound frequency tuning, quite in contrast to the large literature studying this property at the single neuron level. The few existing studies either quantified frequency tuning exclusively in the evoked response (Ohl et al. 2000), or in the lowest frequencies of the LFP (Norena and Eggermont 2002), or they did not systematically quantify tuning properties (Brosch et al. 2002). As a result we know relatively little about the relationship of sound frequency tuning at the level of individual neurons and at the level of local population responses. This is in sharp contrast to research in vision, where several

systematic studies demonstrated that evoked and local field potentials in V1 and MT exhibit tuning to the prominent features represented in these areas (Bonds 1982; Kayser and Konig 2004; Liu and Newsome 2006; Siegel and Konig 2003). Interestingly, these studies reported somewhat differing results: while the V1 studies suggest that feature tuning can be prominent both in lower and higher frequency bands of LFPs, the MT study reported a dissociation of lower and higher LFP frequency bands, with only the latter having comparable tuning to the spiking activity.

The goal of the present study was to obtain a systematic account of sound frequency tuning in neuronal spiking activity as well as in local population responses obtained from the same recording sites. Especially, we wondered whether tuning relationship between neural spiking activity and the LFP follows a similar pattern as observed in one of the visual areas.

We recorded from the auditory cortex from two adult rhesus monkeys that were passively listening to the acoustical stimuli in a sound attenuated booth (Illbruck acoustic GmbH). During recording the animals were awake and not sleeping (as assessed using an infra-red camera and investigation of low-frequency oscillations in the LFP). All procedures were approved by the local authorities (Regierungspräsidium) and were in full compliance with the guidelines of the European Community (EUVD 86/609/EEC). Signals were recorded using commercial microelectrodes (0.8 – 1.2 MOhm impedance), high-pass filtered above 4Hz and low-pass filtered below 10kHz. Sounds (65 dB SPL) were delivered from two free field speakers (JBL Professional, Northridge, CA, 70 cm from the ear, 50 degrees to left and right), which have been calibrated to ensure a linear transfer function (condenser microphone, Brüel & Kjær GmbH, Bremen, Germany). Stimuli consisted of band-passed noise (7 center frequencies from 177Hz to 11'314Hz, one octave steps) and pure tones (15 tones, 125 Hz to 16kHz, half-octave steps). Both were presented as sequences of 8 repeats (50msec sound duration, 80msec inter-sound spacing).

From the recorded signals, the following measures of neuronal activity were extracted. The *Auditory evoked potential (AEP)* was obtained by low-pass filtering the raw data at 150 Hz (3rd order Butterworth filter), and computing the area under this slow wave during a temporal window of interest. The *Local field potential (LFP)* was obtained by convolving individual trials with Gabor wavelets of different center frequencies (5, 10, 20, 40, 60, 80, 120Hz, and a bandwidth of 0.83). The amplitude of this convolution yields an estimate of the signal power in each frequency band. The *Analog multi-unit activity (AMUA)* was obtained by band-pass filtering the raw signal between 500Hz and 3'000 Hz, taking the absolute value and subsequent low-pass filtering at 300Hz. To obtain units that are comparable across recording

sites, these signals were normalized to units of standard deviations from baseline (Logothetis et al. 2001). *Spike-sorted activity (S/MUA)* was extracted using commercial spike-sorting software (Plexon Inc, USA) after high-pass filtering the raw signal at 500 Hz. To contrast the spike-sorted activity versus the other population measures of activity, we grouped single- and multi-unit sites into one category, which we abbreviate S/MUA. For the present study we only analyzed recording sites that responded significantly ($p < 0.05$) to the stimulus, both in the AEP and the spiking activity: the response amplitude during baseline (-200 msec to -20 msec before stimulus onset) was compared to the amplitude after stimulus onset (20 msec to 200 msec) using a paired t-test. Of a total of 258 sites, 119 were determined as responsive. Based on stereotaxic coordinates, frequency maps constructed for each animal as well as responsiveness for tone vs. band-passed stimuli, most of our recording sites were in primary auditory cortex (fields A1 and R, 71 sites) and in the caudal belt (fields CM and CL, 48 sites).

Figure 1A shows examples responses for the different measures of activity and the right panel displays tuning curves for each measure obtained during a window during the initial transient response (20 msec to 200 msec after stimulus onset). This recording site preferred frequencies between 1-2kHz, which was identified as the best frequency (BF) by each activity measure. To quantify the similarity of these tuning curves, we computed the correlation of the S/MUA tuning curve with the tuning curve obtained from each of the other measures. The results (AEP: 0.39, LFP 20, 60 and 120Hz: 0.82, 0.74 and 0.93; AMUA: 0.99) suggest that each activity measure shows tuning to sound frequency, but with varying similarity to the tuning curve obtained from the spike-sorted activity.

Figure 1 about here

The population data (Fig. 2) confirm that this example was typical. Panel 2A shows the BF-difference from each activity measure to BF obtained from the S/MUA. The average difference for the AEP was 2.0 octaves, which was significantly larger than for the AMUA (0.83 octaves, $p < 10^{-4}$). For the LFP there was a systematic trend: the BF-difference decreased with increasing LFP frequency. To quantify this dissociation between low and high LFP frequencies, we directly compared these (paired t-test, 5-40Hz vs. 60-120Hz). The significant difference ($p < 10^{-4}$) demonstrates that the high frequency LFP better represents the tuning properties of the spiking activity than does the low frequency LFP.

Figure 2 about here

Complementing the BF analysis, we computed the similarity (correlation) between the tuning curves obtained from the different activity measures (Fig. 2B). For the AEP, the correlation with the S/MUA tuning curve was significantly lower than for the AMUA ($p < 10^{-7}$). For the LFP there was a systematic trend of increasing correlation with increasing LFP frequency again resulting in a significant difference between the high and low frequency LFP ($p < 10^{-8}$). The magnitude of this correlation depends on the number of measured points and the number of averages contributing to a smooth estimate of the curve. To deal with these limitations, we also compared tuning curves after fitting each individual curve with a Gaussian model (see Liu and Newsome 2006 for a similar approach). As expected, the resulting correlations were indeed higher (mean correlation across all activity measures 0.57 compared to 0.39). But again, the low frequency LFP showed a significantly lower correlation with the spiking activity compared to the high frequency LFP ($p < 0.01$).

Finally, we computed the mutual information between response and stimulus identity (Borst and Theunissen 1999; Panzeri and Treves 1996) (Fig. 2C). With 7 stimuli, the maximal possible information is 2.8 bit. However, as most tuning curves have two flanks (c.f. Fig. 1), the number of actually distinguishable frequencies and the mutual information are usually smaller. Both measures of spiking activity provided similar information (S/MUA: 0.57 bit, AMUA: 0.55 bit, $p > 0.05$), which was significantly higher than the information in the AEP (0.47 bit, $p < 10^{-3}$). In addition, the information conveyed by the LFP was significantly lower compared to the spiking activity (at least $p < 0.05$, see Fig. 2C), and again the low and high LFP components differed significantly ($p < 10^{-6}$).

As the above analysis focused only on the initial transient response, we verified that our findings do not depend on this choice of temporal window: The same analysis was repeated using one window immediately following the first (+200 msec to +380 msec) and one window during the sustained response (+600 msec to +780 msec). Analysis of these confirmed all of the observed findings (Fig. 2D demonstrates this for the similarity of tuning curves).

In addition, we compared the results between the auditory core and belt. The correlation of tuning curves (paired t-test $p = 0.2$) and the BF-difference to the spiking activity ($p = 0.045$) showed only a small difference between these areas (Fig. 2A, B). Comparing the difference of information between the spiking activity and the other measures, however, revealed a significant difference: in the belt, population responses conveyed more information about the stimulus identity ($p < 0.01$). The latter result might be due to our choice of stimulus,

band-passed noise, as it is known that neurons in the belt respond to this stimulus better than neurons in the core.

In contrast to previous studies (Brosch et al. 2002; Norena and Eggermont 2002; Ohl et al. 2000) the present work provides a systematic comparison of sound frequency tuning in several measures of neuronal activity. In contrast to what might be expected from these reports, our results demonstrate that low frequency oscillations and evoked potentials reflect the tuning properties of the neuronal spiking activity to a lesser degree than the high frequency LFP. While this result contrasts somewhat previous findings in the primary visual cortex (Bonds 1982; Kayser and Konig 2004; Siegel and Konig 2003), they fit well with findings from visual area MT (Liu and Newsome 2006), suggesting that the higher frequencies of the LFP in general have a closer relationship to neuronal spiking activity. It should be noted that our results are not a trivial consequence of the higher LFP bands directly reflecting the spiking activity on the same electrode. At least for frequencies up to 120Hz, the LFP can be stimulus selective even in the absence of clear spiking activity (see Supplemental Figure).

There are several reasons why the tuning of the low frequency LFP might be less specific. Previous studies suggested that the cortical tissue might act as a capacitive filter, which allows lower frequencies to travel long distances while attenuating high frequencies (Bedard et al. 2006; Ranck 1963). This would 'blur' the low frequency signals and reduce their selectivity (Liu and Newsome 2006). However, there is good evidence that this is not the case; in fact, the impedance spectrum of cortex is flat (N. Logothetis, manuscript in preparation). As an alternative, it could be that the neuronal sources generating low and high frequency rhythms themselves have a different size. While high frequency signals are likely to originate from localized neuronal clusters (below the scale of a cortical column), low frequency oscillations might be driven by divergent ascending input from the thalamus and brainstem (including neuromodulatory projections). Such difference in the generators is a likely explanation for both, the varying spatial correlation of low and high frequency LFPs (Eckhorn et al. 1988), and their differences in sound frequency tuning.

In addition, previous studies that carefully quantified the tuning properties of neurons in auditory cortex found a considerable heterogeneity, even between neurons recorded on the same electrode (Recanzone et al. 2000): while the center frequencies closely matched, other properties like response thresholds and tuning width differed. Pooling neurons with such varying properties is likely to result in population tuning curves that do not perfectly correlate with those of single neurons. In combination with the varying extent of spatial pooling, this

likely explains the pattern of correlations between different response measures observed in the present study.

Our findings have several implications for auditory activation patterns acquired in functional imaging studies. Work on the neuronal basis of fMRI-BOLD imaging demonstrated a good match between the LFP and the imaging signal (Logothetis and Wandell 2004). In particular, high frequency oscillatory activity, i.e. frequency bands between 40-130 Hz (Logothetis et al. 2001) and 50-90Hz (Niessing et al. 2005), showed a good correspondence to the BOLD signal. Interestingly, in the present study these high frequencies of the LFP showed stronger sound frequency tuning than the low frequency components. Together with the finding that the BOLD signal also correlates with spiking activity (although sometimes to a weaker degree than the LFP), these results suggest that frequency maps of auditory cortex obtained using fMRI should closely correspond to the sound selectivity of the underlying neuronal populations (Formisano et al. 2003; Petkov et al. 2006; Talavage et al. 2004; Wessinger et al. 1997).

Acknowledgements

This work was supported by the Max-Planck Society, the German Research Foundation and the Alexander von Humboldt Foundation.

Figure legend

Figure 1: Example data from one recording site

Left) Response time course for each activity measure analyzed (AEP: auditory evoked potential, LFP: local-field potentials, AMUA: analog multi-unit activity, S/MUA spike sorted single- or multi-unit activity). Shown is the mean response across all sound frequencies. For the LFP each gray level displays a different LFP frequency band; otherwise black lines indicate the mean and gray lines indicate the 99% confidence interval (bootstrap estimate). The S/MUA has units of spikes/second, the other measures have units of z-scores from baseline. The gray box indicates the time window, for which the tuning curves are shown on the right.

Right) Mean and s.e.m. of the response for each sound frequency band of the broad-band noise stimulus. For the S/MUA, the dashed line indicates the baseline response before stimulus presentation (for the other measures the baseline is zero).

Figure 2: Population results

A) Difference of the best frequency (BF) obtained from each activity measure to the BF obtained from the S/MUA.

B) Correlation coefficient between the tuning curves obtained from S/MUA and the other activity measures.

C) Mutual information between response and stimulus identity.

In each panel, circles indicate the mean value (across all sites) and vertical bars indicate its 99% confidence interval (bootstrap estimate). In addition, small gray circles and boxes indicate the mean values separately for recording sites in the core and belt regions. Stars on the bottom indicate the significance of a sign-test between the respective measure and the AMUA or S/MUA (as indicated by the arrow): * $p < 0.05$, ** $p < 0.01$, *** at least $p < 0.001$, all Bonferoni corrected for multiple comparisons.

References

- Bedard C, Kroger H, and Destexhe A.** Model of low-pass filtering of local field potentials in brain tissue. *Phys Rev E Stat Nonlin Soft Matter Phys* 73: 051911, 2006.
- Bonds AB.** An "oblique effect" in the visual evoked potential of the cat. *Exp Brain Res* 46: 151-154, 1982.
- Borst A, and Theunissen FE.** Information theory and neural coding. *Nat Neurosci* 2: 947-957, 1999.
- Brosch M, Budinger E, and Scheich H.** Stimulus-related gamma oscillations in primate auditory cortex. *J Neurophysiol* 87: 2715-2725, 2002.
- Eckhorn R, Bauer R, Jordan W, Brosch M, Kruse W, Munk M, and Reitboeck HJ.** Coherent oscillations: a mechanism of feature linking in the visual cortex? Multiple electrode and correlation analyses in the cat. *Biol Cybern* 60: 121-130, 1988.
- Formisano E, Kim DS, Di Salle F, van de Moortele PF, Ugurbil K, and Goebel R.** Mirror-symmetric tonotopic maps in human primary auditory cortex. *Neuron* 40: 859-869, 2003.
- Freeman W.** Mass action in the nervous system. *Academic Press, New York* 1975.
- Hubel D, and Wiesel TN.** Receptive fields, binocular interaction and functional architecture in the cat's visual cortex. *J Physiol* 160: 106-154, 1962.
- Kaas JH, Hackett TA, and Tramo MJ.** Auditory processing in primate cerebral cortex. *Curr Opin Neurobiol* 9: 164-170, 1999.
- Kayser C, and Konig P.** Stimulus locking and feature selectivity prevail in complementary frequency ranges of V1 local field potentials. *Eur J Neurosci* 19: 485-489, 2004.
- Lauritzen M.** Relationship of spikes, synaptic activity, and local changes of cerebral blood flow. *J Cereb Blood Flow Metab* 21: 1367-1383, 2001.
- Liu J, and Newsome WT.** Local field potential in cortical area MT: stimulus tuning and behavioral correlations. *J Neurosci* 26: 7779-7790, 2006.
- Logothetis NK, Pauls J, Augath M, Trinath T, and Oeltermann A.** Neurophysiological investigation of the basis of the fMRI signal. *Nature* 412: 150-157, 2001.
- Logothetis NK, and Wandell BA.** Interpreting the BOLD Signal. *Annu Rev Physiol* 66: 735-769, 2004.
- Merzenich MM, and Brugge JF.** Representation of the cochlear partition of the superior temporal plane of the macaque monkey. *Brain Res* 50: 275-296, 1973.
- Niessing J, Ebisch B, Schmidt KE, Niessing M, Singer W, and Galuske RA.** Hemodynamic signals correlate tightly with synchronized gamma oscillations. *Science* 309: 948-951, 2005.
- Norena A, and Eggermont JJ.** Comparison between local field potentials and unit cluster activity in primary auditory cortex and anterior auditory field in the cat. *Hear Res* 166: 202-213, 2002.
- Ohl FW, Scheich H, and Freeman WJ.** Topographic analysis of epidural pure-tone-evoked potentials in gerbil auditory cortex. *J Neurophysiol* 83: 3123-3132, 2000.
- Panzeri S, and Treves A.** Analytical estimates of limited sampling biases in different information measures. *Network: Computation in Neural Systems* 7: 87-107, 1996.
- Petkov CI, Kayser C, Augath M, and Logothetis NK.** Functional Imaging Reveals Numerous Fields in the Monkey Auditory Cortex. *PLoS Biol* 4: e215, 2006.
- Ranck JB, Jr.** Specific impedance of rabbit cerebral cortex. *Exp Neurol* 7: 144-152, 1963.
- Rauschecker JP, Tian B, Pons T, and Mishkin M.** Serial and parallel processing in rhesus monkey auditory cortex. *J Comp Neurol* 382: 89-103, 1997.
- Recanzone GH, Guard DC, and Phan ML.** Frequency and intensity response properties of single neurons in the auditory cortex of the behaving macaque monkey. *J Neurophysiol* 83: 2315-2331, 2000.

Siegel M, and Konig P. A functional gamma-band defined by stimulus-dependent synchronization in area 18 of awake behaving cats. *J Neurosci* 23: 4251-4260, 2003.

Talavage TM, Sereno MI, Melcher JR, Ledden PJ, Rosen BR, and Dale AM. Tonotopic organization in human auditory cortex revealed by progressions of frequency sensitivity. *J Neurophysiol* 91: 1282-1296, 2004.

Wessinger CM, Buonocore MH, Kussmaul CL, and Mangun GR. Tonotopy in human auditory cortex examined with functional magnetic resonance imaging. *Neuroimage* 5: 18-25, 1997.

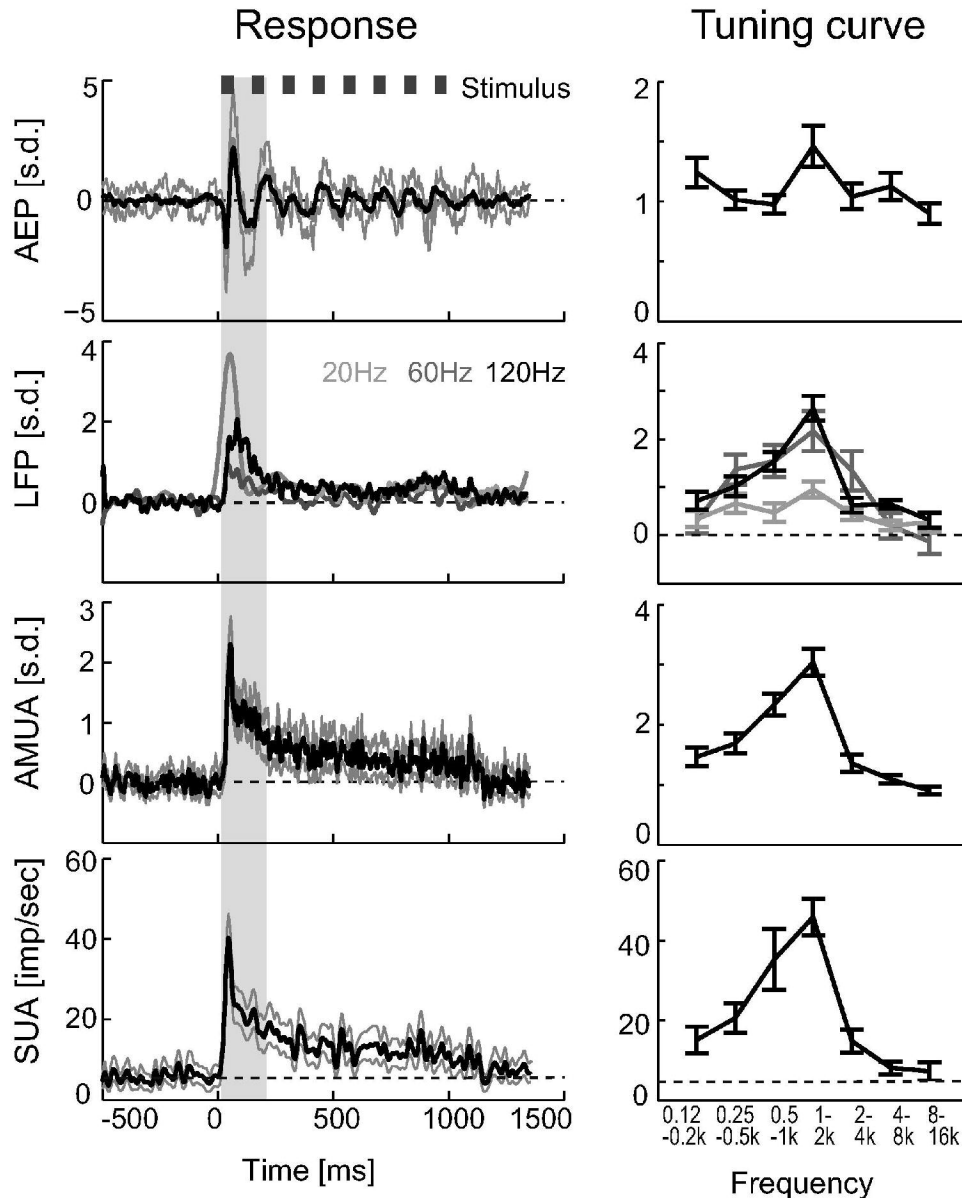


Figure 1: Example data from one recording site Left) Response time course for each activity measure analyzed (AEP: auditory evoked potential, LFP: local-field potentials, AMUA: analog multi-unit activity, S/MUA spike sorted single- or multi-unit activity). Shown is the mean response across all sound frequencies. For the LFP each gray level displays a different LFP frequency band; otherwise black lines indicate the mean and gray lines indicate the 99% confidence interval (bootstrap estimate). The S/MUA has units of spikes/second, the other measures have units of z-scores from baseline. The gray box indicates the time window, for which the tuning curves are shown on the right. Right) Mean and s.e.m. of the response for each sound frequency band of the broad-band noise stimulus. For the S/MUA, the dashed line indicates the baseline response before stimulus presentation (for the other measures the baseline is zero).

82x103mm (600 x 600 DPI)

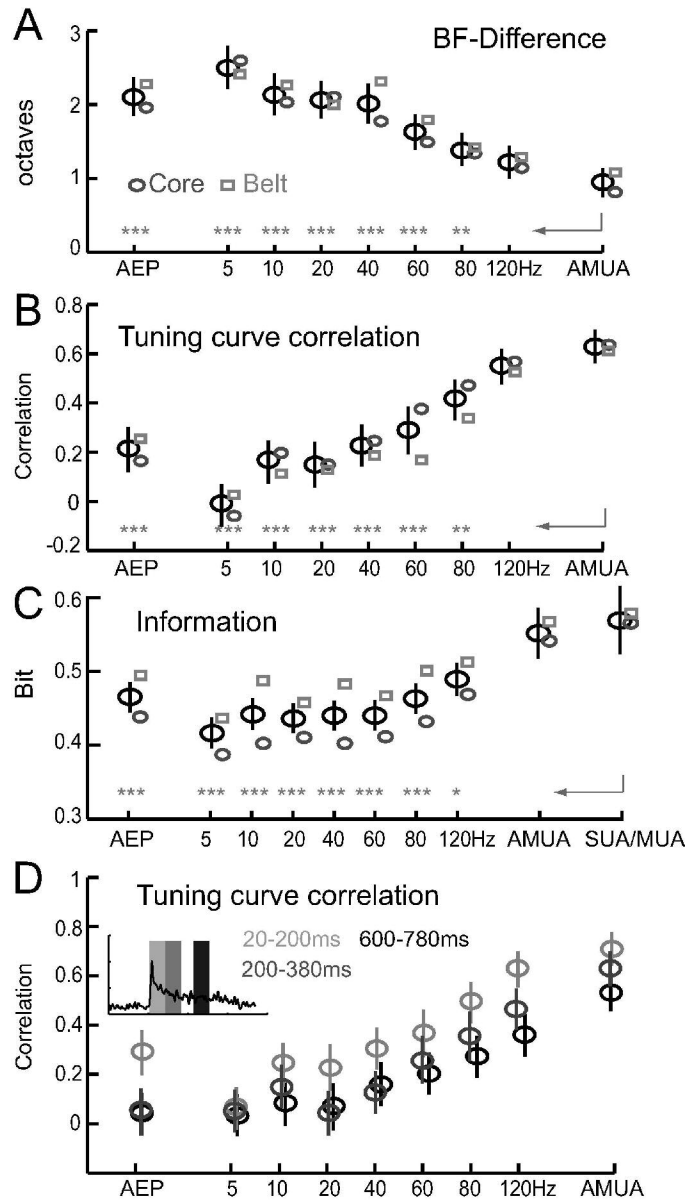


Figure 2: Population results A) Difference of the best frequency (BF) obtained from each activity measure to the BF obtained from the S/MUA. B) Correlation coefficient between the tuning curves obtained from S/MUA and the other activity measures. C) Mutual information between response and stimulus identity. In each panel, circles indicate the mean value (across all sites) and vertical bars indicate its 99% confidence interval (bootstrap estimate). In addition, small gray circles and boxes indicate the mean values separately for recording sites in the core and belt regions. Stars on the bottom indicate the significance of a sign-test between the respective measure and the AMUA or S/MUA (as indicated by the arrow): * $p < 0.05$, ** $p < 0.01$, *** at least $p < 0.001$, all Bonferoni corrected for multiple comparisons.

75x134mm (600 x 600 DPI)

